

A comparison of deep networks with ReLU activation function and linear spline-type methods

Konstantin Eckle *

Johannes Schmidt-Hieber *

Abstract

Deep neural networks (DNNs) generate much richer function spaces than shallow networks. Since the function spaces induced by shallow networks have several approximation theoretic drawbacks, this explains, however, not necessarily the success of deep networks. In this article we take another route by comparing the expressive power of DNNs with ReLU activation function to piecewise linear spline methods. We show that MARS (multivariate adaptive regression splines) is improperly learnable by DNNs in the sense that for any given function that can be expressed as a function in MARS with M parameters there exists a multilayer neural network with $O(M \log(M/\varepsilon))$ parameters that approximates this function up to sup-norm error ε . We show a similar result for expansions with respect to the Faber-Schauder system. Based on this, we derive risk comparison inequalities that bound the statistical risk of fitting a neural network by the statistical risk of spline-based methods. This shows that deep networks perform better or only slightly worse than the considered spline methods. We provide a constructive proof for the function approximations.

AMS 2010 Subject Classification: Primary 62G08; secondary 62G20.

Keywords: Deep neural networks; nonparametric regression; splines; MARS; Faber-Schauder system; rates of convergence.

1 Introduction

Training of DNNs is now state of the art for many different complex tasks including detection of objects on images, speech recognition and game playing. For these modern applications, the ReLU activation function is standard. One of the distinctive features of a multilayer neural network with ReLU activation function is that the output is always a piecewise linear function of the input. But there are also other well-known

*Leiden University, Mathematical Institute, Niels Bohrweg 1, 2333 CA Leiden, The Netherlands, k.j.eckle@math.leidenuniv.nl; schmidthieberaj@math.leidenuniv.nl

nonparametric estimation techniques that are based on function systems build from piecewise linear functions. This raises the question in which sense these methods are comparable.

Deep networks outperform shallow networks in the sense that the function classes are much richer, cf. [10, 2, 14, 16, 9, 12]. In terms of function systems, shallow networks have, however, several drawbacks. It requires many nodes/units to localize and to approximate for instance a function supported on a smaller hypercube. Moreover, shallow networks need a large number of parameters to approximately multiply inputs. To explain the success of deep networks, it is therefore natural to compare them with methods that do not suffer from these shortcomings.

In this article, we compare deep networks to multivariate adaptive regression splines (MARS) [4] and to series expansions with respect to the Faber-Schauder system [3, 15]. MARS is a widely applied method in statistical learning [7]. Similar as multilayer neural networks, MARS builds functions from simple objects and has width and depth like parameters. Compared to DNNs, MARS also uses multiplications to generate functions. The Faber-Schauder functions are the integrals of the Haar wavelet functions and are hence piecewise linear. Series expansion with respect to the Faber-Schauder system result in a piecewise linear approximation. Both MARS and Faber-Schauder system satisfy an universal approximation theorem, see Section 2.2 for a discussion.

We show that for any given function that can be expressed as a function in MARS or the Faber-Schauder basis with M parameters there exists a multilayer neural network with $O(M \log(M/\varepsilon))$ parameters that approximates this function up to sup-norm error ε . We also show that the opposite is false. There are functions that can be approximated up to error ε with $O(\log(1/\varepsilon))$ network parameters but require at least $O(1/\sqrt{\varepsilon})$ many parameters if approximated by MARS or the Faber-Schauder system.

The result provides a simple route to establish approximation properties of deep networks. For the Faber-Schauder system, approximation rates can often be deduced in a straightforward way and these rates then carry over immediately to approximations by deep networks. As another application, we prove that for nonparametric regression, fitting a DNN will never have a much larger risk than MARS or series expansion with respect to the Faber-Schauder system.

The proof of the approximation of MARS and Faber-Schauder functions by multilayer neural network is constructive. This allows to run a two-step procedure which in a first step estimates/learns a MARS or Faber-Schauder function. This is then used to initialize the DNN. For more details see Section 4.1.

Related to our work, there are few results in the literature which show that the class of function generated by multilayer neural networks can be embedded into a larger space. [17] shows that neural network functions are also learnable by a carefully designed kernel method. Unfortunately, the analysis relies on a power series expansion of the activation function and does not hold for the ReLU. In [18], a convex relaxation of convolutional neural networks is proposed and a risk bound is derived.

This paper is organized as follows. Section 2 provides short introductions to the construction of MARS functions and Faber-Schauder systems. Notation and basic results for DNNs are summarized in Section 3. Section 4 contains the main results on approximation of MARS and Faber-Schauder functions by DNNs. In Section 5, we derive risk comparison inequalities for nonparametric regression. Numerical simulations can be found in Section 6. Additional proofs are deferred to the end of the article.

Notation: Throughout the paper, vectors are displayed by bold letters, e.g. \mathbf{X}, \mathbf{x} .

2 Spline type methods for function estimation

In this section, we describe MARS and expansions with respect to the Faber-Schauder system. For both methods we discuss the underlying function space and algorithms that fit the function system to a dataset.

2.1 MARS - Multivariate Adaptive Regression Splines

Consider functions of the form

$$h_{I,\mathbf{t}}(x_1, \dots, x_d) = \prod_{j \in I} (s_j(x_j - t_j))_+, \quad \mathbf{x} = (x_1, \dots, x_d)^\top \in [0, 1]^d, \quad (1)$$

with $I \subseteq \{1, \dots, d\}$ an index set, $s_j \in \{-1, 1\}$ and $\mathbf{t} = (t_j)_{j \in I} \in [0, 1]^{|I|}$ a shift vector. These are piecewise linear functions in each argument, and the supports of the functions are hyperrectangles. Suppose we want to find a linear combination of functions $h_{I,\mathbf{t}}$ that best explains the data. To this end, we would ideally minimize the least-squares functional over all possible linear combinations of at most M of these functions, where M is a predetermined cut-off parameter. In other words, we consider least-squares optimization over the following function class.

Definition 2.1. *For any positive integer M and any constant $C > 0$, define the family of functions*

$$\mathcal{F}_{\text{MARS}}(M, C) = \left\{ \mathbf{x} \mapsto \beta_0 + \sum_{m=1}^M \beta_m h_m(\mathbf{x}) : h_m \text{ is of the form (1), } |\beta_m| \leq C \right\},$$

with $\mathbf{x} \in [0, 1]^d$. We further assume that $\|f\|_\infty \leq F$ for all $f \in \mathcal{F}_{\text{MARS}}(M, C)$ for some $F > 0$.

Approximating a function f by a linear combination of MARS functions allows to take advantage of low-dimensional structures such as an additive decomposition $f(\mathbf{x}) = \sum_{i=1}^d f_i(x_i)$. In Section 4.2, we show that there are also functions that are very hard to approximate with respect to the MARS function system.

Least-squares minimization over the whole function space is, however, computationally intractable. Instead, MARS - proposed by [4] - is a greedy algorithm that searches for a set of basis functions $h_{I,\mathbf{t}}$ that explain the data well. Starting with the constant function, in each step of the procedure two basis functions are added. The new basis functions are products of an existing basis function with a new factor $(x_j - t_j)_+$, where t_j coincides with the j -th component of one of the design vectors. Among all possible choices, the basis functions that lead to the best least-squares fit are selected. The algorithm is stopped after a prescribed number of iterations. It can be appended by a backwards deletion procedure that iteratively deletes a fixed number of selected basis functions with small predictive power. Algorithm 1 provides additional details. In the original article [4] the values for t_j are restricted to a smaller set.

Input : Integer M' and sample (\mathbf{X}_i, Y_i) , $i = 1, \dots, n$
Output: $2M' + 1$ basis functions of the form (1)
 $\mathcal{S} \leftarrow \{1\}$
for k from 1 to M' **do**
 for $g \in \mathcal{S}$ **do**
 $J(g) \leftarrow \{j : x_j \mapsto g(x_1, \dots, x_d) \text{ is constant}\}$
 end
 $(g^*, j^*, t_{j^*}^*) \leftarrow \text{argmin over } g \in \mathcal{S}, j \in J(g), t_j \in \{X_{ij}, i = 1, \dots, n\} \text{ of the least squares fits for the models } \mathcal{S} \cup \{\mathbf{x} \mapsto (x_j - t_j)_+ g(\mathbf{x}), \mathbf{x} \mapsto (t_j - x_j)_+ g(\mathbf{x})\}.$
 $\mathcal{S} \leftarrow \mathcal{S} \cup \{\mathbf{x} \mapsto (x_{j^*} - t_{j^*}^*)_+ g^*(\mathbf{x}), \mathbf{x} \mapsto (t_{j^*}^* - x_{j^*})_+ g^*(\mathbf{x})\}.$
end
return \mathcal{S}

Algorithm 1: MARS forward selection

The least squares functional can also be replaced by another loss. The runtime of the algorithm is of the order $(M')^3 nd$, where the key step is the computation of the argmin which is easily parallelizable. [5] considers a variation of the MARS procedure where the runtime dependence on M' is only quadratic.

There are many higher-order generalization of the MARS procedure. E.g., [4] proposed also to use truncated power basis functions

$$(s_j(x_j - t_j))_+^q, \quad q \in \mathbb{N},$$

to represent q th order splines. Another common generalization of the MARS algorithm allows for piecewise polynomial basis functions in each argument of the form

$$h_{K,\mathbf{t}}(x_1, \dots, x_d) = \prod_{j=1}^K (s_j(x_{i(j)} - t_j))_+, \quad K \in \mathbb{N}, s_j \in \{-1, 1\}, \mathbf{t} \in [0, 1]^K, \quad (2)$$

where $i(\cdot)$ is a mapping $\{1, \dots, K\} \rightarrow \{1, \dots, d\}$. The theoretical results of this paper can be generalized in a straightforward way to these types of higher-order basis functions. If the MARS algorithm is applied to the function class generated by (2), we refer to this as higher order MARS (HO-MARS).

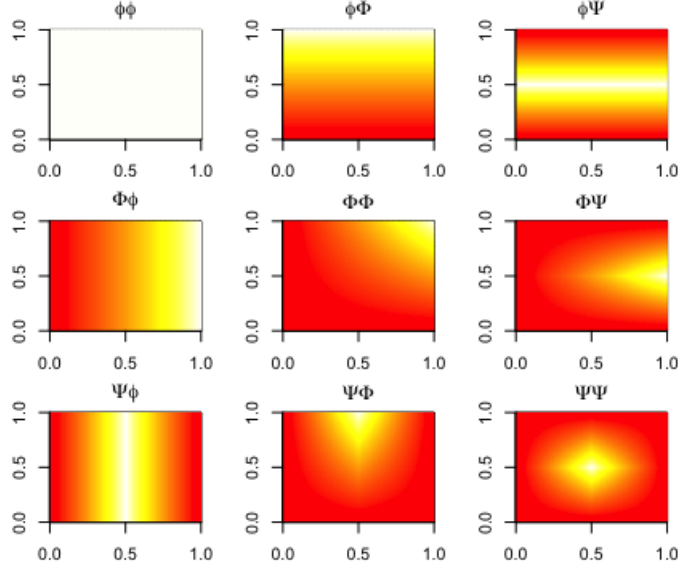


Figure 1: First functions of the bivariate Faber-Schauder system displayed as heatmaps.

2.2 The Faber-Schauder system

The Faber-Schauder system defines a family of functions $[0, 1]^d \rightarrow \mathbb{R}$ that can be viewed as the system of indefinite integrals of the Haar wavelet functions. Faber-Schauder functions are piecewise linear in each component and expansion with respect to the Faber-Schauder system results therefore in (componentwise) piecewise linear approximations.

To describe the expansion of a function with respect to the Faber-Schauder system, consider first the univariate case $d = 1$. Let $\phi(x) = x$ and $\psi = \mathbb{1}(\cdot \in [0, 1/2)) - \mathbb{1}(\cdot \in [1/2, 1])$. The Haar wavelet consists of the functions $\{\phi, \psi_{j,k}, j = 0, 1, \dots; k = 0, \dots, 2^j - 1\}$ with $\psi_{j,k} = 2^{j/2}\psi(2^j \cdot -k)$.

Define $\Phi(x) = \int_0^x \phi(u) du = x$ and $\Psi_{j,k}(x) = \int_0^x \psi_{j,k}(u) du$. The functions $\Psi_{j,k}$ are triangular functions on the interval $[k2^{-j}, (k+1)2^{-j}]$. The Faber-Schauder system on $[0, 1]$ is $\{\phi, \Phi, \Psi_{j,k}, j = 0, 1, \dots; k = 0, \dots, 2^j - 1\}$.

Lemma 2.2. *Let f be a function in the Sobolev space $\{f : f' \in L^2[0, 1]\}$. Then,*

$$f(x) = f(0) + (f(1) - f(0))x + \sum_{j=0}^{\infty} \sum_{k=0}^{2^j-1} d_{j,k} \Psi_{j,k}(x)$$

with $d_{j,k} = -2^{j/2}(f(\frac{k+1}{2^j}) - 2f(\frac{k+1/2}{2^j}) + f(\frac{k}{2^j}))$ and convergence of the sum in $L^2[0, 1]$.

Proof. It is well-known that the Haar wavelet generates an orthonormal basis of $L^2[0, 1]$.

Since by assumption $f' \in L^2[0, 1]$,

$$f'(x) = f(1) - f(0) + \sum_{j=0}^{\infty} \sum_{k=0}^{2^j-1} d_{j,k} \psi_{j,k}(x)$$

with $d_{j,k} = \int f'(u) \psi_{j,k}(u) du = -2^{j/2}(f(\frac{k+1}{2^j}) - 2f(\frac{k+1/2}{2^j}) + f(\frac{k}{2^j}))$ and convergence in $L^2[0, 1]$. The result follows by integrating both sides together with the fact that $\|h\|_{L^2[0,1]} \leq \|h'\|_{L^2[0,1]}$ whenever $h' \in L^2[0, 1]$. \square

In the univariate case, expansion with respect to the Faber-Schauder system is the same as piecewise linear interpolation on a dyadic grid. On the lowest resolution level, the function f is approximated by $f(0) + (f(1) - f(0))x$ which interpolates the function at $x = 0$ and $x = 1$. If we go up to the j -th resolution level, the Faber-Schauder reconstruction linearly interpolates the function f on the dyadic grid $x = k/2^{j+1}$, $k = 0, 1, \dots, 2^{j+1}$. The Faber-Schauder system is consequently also a basis for the continuous functions equipped with the uniform norm. In neural networks terminology, this means that an universal approximation theorem holds for the Faber-Schauder system.

The multivariate Faber-Schauder system can be obtained by tensorization. Let $\Psi_{-2} := \phi$, $\Psi_{-1} := \Phi$, $\Lambda_\ell := \{-2, -1, (j, k), j = 0, 1, \dots, \ell; k = 0, \dots, 2^j - 1\}$, and $\Lambda = \Lambda_\infty$. Then, we can rewrite the univariate Faber-Schauder system on $[0, 1]$ as $\{\Psi_\lambda : \lambda \in \Lambda\}$. The d -variate Faber-Schauder system on $[0, 1]^d$ consists of the functions

$$\{\Psi_{\lambda_1} \otimes \dots \otimes \Psi_{\lambda_d} : \lambda_i \in \Lambda\}.$$

In the following, we write $\boldsymbol{\lambda}$ for the vector $(\lambda_1, \dots, \lambda_d)$. Given $\boldsymbol{\lambda} = (\lambda_1, \dots, \lambda_d)$, let $I(\boldsymbol{\lambda})$ denote the set containing all indices with $\lambda_i \neq -2$. Given an index set $I \subseteq \{1, \dots, d\}$, $f(0_{I^c}, u_I)$ denotes the function f with components in $I^c = \{1, \dots, d\} \setminus I$ being zero. Moreover, for $I = \{i_1, \dots, i_\ell\}$, $\partial_I = \partial_{i_1} \dots \partial_{i_\ell}$ stands for the partial derivative with respect to the indices i_1, \dots, i_ℓ . Let also $\psi_{-1} := \phi$.

Lemma 2.3. *Suppose that for all sets $I \subseteq \{1, \dots, d\}$, $\partial_I f(0_{I^c}, u_I) \in L^2[0, 1]^{|I|}$. Then, with $\boldsymbol{x} = (x_1, \dots, x_d) \in [0, 1]^d$,*

$$f(\boldsymbol{x}) = \sum_{\boldsymbol{\lambda} \in \Lambda \times \dots \times \Lambda} d_{\boldsymbol{\lambda}} \Psi_{\lambda_1}(x_1) \cdot \dots \cdot \Psi_{\lambda_d}(x_d)$$

with $d_{\boldsymbol{\lambda}} = \int_0^1 \dots \int_0^1 \partial_{I(\boldsymbol{\lambda})} f(0_{I(\boldsymbol{\lambda})^c}, u_{I(\boldsymbol{\lambda})}) \prod_{i \in I(\boldsymbol{\lambda})} \psi_{\lambda_i}(u_i) du_{i_1} \dots du_{i_\ell}$. The right hand side should be interpreted as $\lim_{\ell \rightarrow \infty} \sum_{\boldsymbol{\lambda} \in \Lambda_\ell \times \dots \times \Lambda_\ell}$ and converges in $L^2([0, 1]^d)$.

Proof. By induction on d ,

$$f(\boldsymbol{x}) = \sum_{I=\{i_1, \dots, i_\ell\} \subseteq \{1, \dots, d\}} \int_0^{x_{i_1}} \dots \int_0^{x_{i_\ell}} \partial_I f(0_{I^c}, u_I) du_{i_1} \dots du_{i_\ell}.$$

Now, we can expand each of the partial derivatives with respect to the Haar wavelet

$$\partial_I f(0_{I^c}, u_I) = \sum_{\boldsymbol{\lambda}=(\lambda_1, \dots, \lambda_\ell) \in (\Lambda \setminus \{-2\})^\ell} d_{\boldsymbol{\lambda}} \psi_{\lambda_1}(u_{i_1}) \cdot \dots \cdot \psi_{\lambda_\ell}(u_{i_\ell})$$

using that $\psi_{-1} := \phi$ and $(\Lambda \setminus \{-2\})^\ell := (\Lambda \setminus \{-2\}) \times \dots \times (\Lambda \setminus \{-2\})$. Convergence is in $L^2[0, 1]^\ell$ for the limit $\lim_{k \rightarrow \infty} \sum_{\boldsymbol{\lambda} \in (\Lambda_k \setminus \{-2\})^\ell}$. Therefore, for $\boldsymbol{x} = (x_1, \dots, x_d) \in [0, 1]^d$,

$$\begin{aligned} f(\boldsymbol{x}) &= \sum_{I=\{i_1, \dots, i_\ell\} \subseteq \{1, \dots, d\}} \sum_{\boldsymbol{\lambda}=(\lambda_1, \dots, \lambda_\ell) \in (\Lambda \setminus \{-2\})^\ell} d_{\boldsymbol{\lambda}} \Psi_{\lambda_1}(x_{i_1}) \cdot \dots \cdot \Psi_{\lambda_\ell}(x_{i_\ell}) \\ &= \sum_{\boldsymbol{\lambda} \in \Lambda \times \dots \times \Lambda} d_{\boldsymbol{\lambda}} \Psi_{\lambda_1}(x_1) \cdot \dots \cdot \Psi_{\lambda_d}(x_d) \end{aligned}$$

using that $\Psi_{-2} = 1$ on $[0, 1]$. □

Because the Haar wavelet functions are piecewise constant, the coefficients $d_{\boldsymbol{\lambda}}$ can also be expressed as a linear combination of function values of f . In particular, we recover for $d = 1$ that $d_{\boldsymbol{\lambda}} = -2^{j/2}(f(\frac{k+1}{2^j}) - 2f(\frac{k+1/2}{2^j}) + f(\frac{k}{2^j}))$ if $\boldsymbol{\lambda} = (j, k)$.

Similarly as in the univariate case, the multivariate Faber-Schauder system interpolates the function on a dyadic grid. Given that $f(\boldsymbol{x}) = \sum_{\boldsymbol{\lambda} \in \Lambda \times \dots \times \Lambda} d_{\boldsymbol{\lambda}} \Psi_{\lambda_1}(x_1) \cdot \dots \cdot \Psi_{\lambda_d}(x_d)$, let

$$T_\ell f(\boldsymbol{x}) = \sum_{\boldsymbol{\lambda} \in \Lambda_\ell \times \dots \times \Lambda_\ell} d_{\boldsymbol{\lambda}} \Psi_{\lambda_1}(x_1) \cdot \dots \cdot \Psi_{\lambda_d}(x_d).$$

It can be shown that $T_\ell f(\boldsymbol{x}) = f(\boldsymbol{x})$ for all grid points $\boldsymbol{x} = (x_1, \dots, x_d)$ with each component $x_j \in \{k2^{-\ell-1} : k = 0, \dots, 2^{\ell+1}\}$. Since $T_\ell f(\boldsymbol{x})$ is also piecewise linear in each component, the universal approximation theorem also holds for the multivariate Faber-Schauder system on $[0, 1]^d$.

Definition 2.4. For any non-negative integer M and any constant $C > 0$ the d -variate Faber-Schauder class truncated at resolution level M is defined as

$$\mathcal{F}_{\text{FS}}(M, C) = \left\{ \boldsymbol{x} \mapsto \sum_{\boldsymbol{\lambda} \in \Lambda_M \times \dots \times \Lambda_M} \beta_{\boldsymbol{\lambda}} \Psi_{\lambda_1}(x_1) \cdot \dots \cdot \Psi_{\lambda_d}(x_d) : |\beta_{\boldsymbol{\lambda}}| \leq C \right\}.$$

We further assume that $\|f\|_\infty \leq F$ for all $f \in \mathcal{F}_{\text{FS}}(M, C)$ for some $F > 0$.

The cardinality of the index set Λ_M is $(1+2^{M+1})$. The class $\mathcal{F}_{\text{FS}}(M, C)$ therefore consists of functions with

$$I := (1 + 2^M)^d \tag{3}$$

many parameters. Every function $\Psi_{\lambda_1} \cdot \dots \cdot \Psi_{\lambda_d}$ can be represented as a linear combination of 3^d MARS functions. This yields the following result.

Lemma 2.5. *Let I be defined as in (3). Then, for any $M, C > 0$,*

$$\mathcal{F}_{\text{FS}}(M, C) \subseteq \mathcal{F}_{\text{MARS}}(3^d I, 2^{d(M+2)/2} C).$$

Proof. For $j = 0, 1, \dots, k = 0, \dots, 2^j - 1$,

$$\Psi_{jk}(x) = 2^{j/2} \left(x - \frac{k}{2^j}\right)_+ - 2^{j/2+1} \left(x - \frac{k+1/2}{2^j}\right)_+ + 2^{j/2} \left(x - \frac{k+1}{2^j}\right)_+$$

This shows that any function $\beta_{\boldsymbol{\lambda}} \Psi_{\lambda_1}(x_1) \cdot \dots \cdot \Psi_{\lambda_d}(x_d)$ with $\boldsymbol{\lambda} \in \Lambda_M \times \dots \times \Lambda_M$ can be written as a linear combination of at most 3^d MARS functions with coefficients bounded by $|\beta_{\boldsymbol{\lambda}}| 2^{d(M+2)/2}$. \square

A consequence is that also the MARS functions satisfy an universal approximation theorem.

Reconstruction with respect to the Faber-Schauder system: Given a sample (\mathbf{X}_i, Y_i) , $i = 1, \dots, n$, we can fit the best least-squares Faber-Schauder approximation to the data by solving

$$\hat{f} \in \arg \min_{f \in \mathcal{F}_{\text{FS}}(M, \infty)} \sum_{i=1}^n (Y_i - f(\mathbf{X}_i))^2.$$

The coefficients can be equivalently obtained by the least-squares reconstruction in the linear model $\mathbf{Y} = \mathbb{X}\boldsymbol{\beta} + \boldsymbol{\varepsilon}$ with observation vector $\mathbf{Y} = (Y_1, \dots, Y_n)^\top$, coefficient vector $\boldsymbol{\beta} = (\beta_{\boldsymbol{\lambda}})_{\boldsymbol{\lambda} \in \Lambda_M \times \dots \times \Lambda_M}^\top$ and $n \times I$ design matrix

$$\mathbb{X} = \left(\Psi_{\lambda_1}(X_{i1}) \cdot \dots \cdot \Psi_{\lambda_d}(X_{id}) \right)_{i=1, \dots, n; (\lambda_1, \dots, \lambda_d) \in \Lambda_M \times \dots \times \Lambda_M}.$$

The matrix \mathbb{X} is sparse because of disjoint supports of the Faber-Schauder functions. The least squares estimate is $\hat{\boldsymbol{\beta}} = (\mathbb{X}^\top \mathbb{X})^{-1} \mathbb{X}^\top \mathbf{Y}$. If $\mathbb{X}^\top \mathbb{X}$ is singular or close to singular, we can employ Tikhonov regularization/ ridge regression leading to $\hat{\boldsymbol{\beta}}_\alpha = (\mathbb{X}^\top \mathbb{X} + \alpha \mathbb{I})^{-1} \mathbb{X}^\top \mathbf{Y}$ with \mathbb{I} the identity matrix and $\alpha > 0$.

For large matrix dimension direct inversion is computationally infeasible. One option is stochastic gradient descent which has a particularly simple form and coincides for this problem with the randomized Kaczmarz method, [11].

3 Deep neural networks (DNNs)

In computer science, DNNs are typically introduced via their representation as directed graphs. For our purposes, it is more convenient to work with the equivalent algebraic definition.

The *number of hidden layers* or *depth* of the multilayer neural network is denoted by L . The *width* of the network is described by a width vector $\mathbf{p} = (p_0, \dots, p_{L+1}) \in \mathbb{N}^{L+2}$ with $p_0 = d$ the input dimension. The *activation function* of the network is the ReLU $\sigma(x) = (x)_+ = \max(x, 0)$, $x \in \mathbb{R}$. For vectors $\mathbf{y} = (y_1, \dots, y_r)$, $\mathbf{v} = (v_1, \dots, v_r) \in \mathbb{R}^r$, define the shifted activation function $\sigma_{\mathbf{v}} : \mathbb{R}^r \rightarrow \mathbb{R}^r$, $\sigma_{\mathbf{v}}(\mathbf{y}) = (\sigma(y_1 - v_1), \dots, \sigma(y_r - v_r))^\top$.

A network is then any function of the form

$$f(\mathbf{x}) = W_{L+1} \circ \sigma_{\mathbf{v}_L} \circ \dots \circ W_2 \circ \sigma_{\mathbf{v}_1} \circ W_1 \mathbf{x}, \quad \mathbf{x} \in \mathbb{R}^d, \quad (4)$$

with $W_\ell \in \mathbb{R}^{p_\ell \times p_{\ell-1}}$ and $\mathbf{v}_\ell \in \mathbb{R}^{p_\ell}$. For convenience, we omit the composition symbol “ \circ ” and write e.g. $f(\mathbf{x}) = W_{L+1} \sigma_{\mathbf{v}_L} \dots W_2 \sigma_{\mathbf{v}_1} W_1 \mathbf{x}$. To obtain networks that are real-valued functions, we must have $p_{L+1} = 1$.

We mainly work with sparsely connected networks. This means that most of the network parameters are zero or non-active. The number of *active/non-zero parameters* is defined as

$$s = \sum_{\ell=1}^{L+1} |W_\ell|_0 + \sum_{\ell=1}^L |\mathbf{v}_\ell|_0,$$

where $|W_\ell|_0$ and $|\mathbf{v}_\ell|_0$ denote the number of non zero entries of the weight matrices W_ℓ and shift vectors \mathbf{v}_ℓ . A fully connected network has

$$s = \sum_{\ell=0}^L (p_\ell + 1)p_{\ell+1} - p_{L+1} \quad (5)$$

active parameters. The function class of all networks with the same network architecture (L, \mathbf{p}) and network sparsity s can then be defined as follows.

Definition 3.1. For $L, s \in \mathbb{N}$ and $\mathbf{p} = (p_0, \dots, p_{L+1}) \in \mathbb{N}^{L+2}$ denote by $\mathcal{F}(L, \mathbf{p}, s)$ the class of neural networks with depth L , width vector \mathbf{p} , number of active parameters s and ReLU activation function, for which the absolute value of all parameters, that is, the entries of W_ℓ and \mathbf{v}_ℓ , are bounded by one. We further assume that $\|f\|_\infty \leq F$ for all $f \in \mathcal{F}(L, \mathbf{p}, s)$ for some $F > 0$.

Fitting a DNN to data is typically done via stochastic gradient descent of the empirical loss. The practical success of DNNs is partially due to a combination of several methods and tricks that are build into the algorithm. An excellent treatment is [6].

4 Deep networks vs. spline type methods

4.1 Improper learning of spline type methods by deep networks

We derive below ReLU network architectures which allow for an approximation of every MARS and Faber-Schauder function up to a small error.

Lemma 4.1. *For fixed input dimension, any positive integer M , any constant C , and any $\varepsilon \in (0, 1]$, there exists (L, \mathbf{p}, s) with*

$$L = O\left(\log \frac{MC}{\varepsilon}\right), \quad \max_{\ell=0, \dots, L+1} p_\ell = O(M), \quad s = O\left(M \log \frac{MC}{\varepsilon}\right),$$

such that

$$\inf_{h \in \mathcal{F}(L, \mathbf{p}, s)} \|f - h\|_\infty \leq \varepsilon \quad \text{for all } f \in \mathcal{F}_{\text{MARS}}(M, C).$$

Recall that $f \in \mathcal{F}_{\text{MARS}}(M, C)$ consists of M basis functions. The neural network h should consequently also have at least $O(M)$ active parameters. The previous result shows that for neural networks we need $O(M \log(M/\varepsilon))$ many parameters. Using DNNs, the number of parameters is thus inflated by a factor $\log(M/\varepsilon)$ that depends on the error level ε .

Recall that $I = (1 + 2^M)^d$. Using the embedding of Faber-Schauder functions into the class of MARS functions given in Lemma 2.5, we obtain as a direct consequence

Lemma 4.2. *For fixed input dimension, any positive integer M , any constant C , and any $\varepsilon \in (0, 1]$, there exists (L, \mathbf{p}, s) with*

$$L = O\left(\log \frac{IC}{\varepsilon}\right), \quad \max_{\ell=0, \dots, L+1} p_\ell = O(I), \quad s = O\left(I \log \frac{IC}{\varepsilon}\right),$$

such that

$$\inf_{h \in \mathcal{F}(L, \mathbf{p}, s)} \|f - h\|_\infty \leq \varepsilon \quad \text{for all } f \in \mathcal{F}_{\text{FS}}(M, C).$$

The number of required network parameters s needed to approximate a Faber-Schauder function with I parameters is thus also of order I up to a logarithmic factor.

The proofs of Lemma 4.1 and Lemma 4.2 are constructive. To find a good initialization of a neural network, we can therefore run MARS in a first step and then use the construction in the proof to obtain a DNN that generates the same function up to an error ε . This DNN is a good initial guess for the true input-output relation and can therefore be used as initialization for any iterative method.

There exists a network architecture which allows to approximate the product of any two numbers in $[0, 1]$ at an exponential rate with respect to the number of network parameters, cf. [16, 13]. This construction is the key step in the approximation theory of DNNs with ReLU activation functions and allows us to approximate the classes of basis functions presented in Section 2. More precisely, we consider the following iterative extension to the product of r numbers in $[0, 1]$.

Lemma 4.3 (Lemma 3 in [13]). *For any $N \geq 1$, there exists a network $\text{Mult}_N^r \in \mathcal{F}((N+5)\lceil \log_2 r \rceil, (r, 6r, 6r, \dots, 6r, 1), s)$ such that $\text{Mult}_N^r(\mathbf{x}) \in [0, 1]$ and*

$$\left| \text{Mult}_N^r(\mathbf{x}) - \prod_{j=1}^r x_j \right| \leq 3^r 2^{-N} \quad \text{for all } \mathbf{x} = (x_1, \dots, x_r) \in [0, 1]^r.$$

By (5) the number of network parameters s is bounded by $42r^2(1 + (N+5)\lceil \log_2 r \rceil)$.

4.2 Lower bounds

In this section, we show that MARS and Faber-Schauder system require much more parameters to approximate the functions $f(x) = x^2$ and $f(x_1, x_2) := (x_1 + x_2 - 1)_+$. This shows that the converse of Lemma 4.1 and Lemma 4.2 is false and also gives some insights when DNNs work better.

The case $f(x) = x^2$: This is an example of a univariate function where DNNs need much fewer parameters compared to MARS and Faber-Schauder system.

Theorem 4.4. *Let $\varepsilon > 0$ and $f(x) = x^2$.*

(i) *If $M \leq 1/(6\sqrt{\varepsilon})$, then*

$$\inf_{g \in \mathcal{F}_{\text{MARS}}(M, \infty)} \|g - f\|_{\infty} \geq \varepsilon.$$

(ii) *If $2^{M+5} \geq 1/\sqrt{\varepsilon}$ then*

$$\inf_{g \in \mathcal{F}_{\text{FS}}(M, \infty)} \|g - f\|_{\infty} \geq \varepsilon.$$

(iii) *There exists a neural network h with $O(\log(1/\varepsilon))$ many layers and $O(\log(1/\varepsilon))$ many network parameters such that*

$$\|h - f\|_{\infty} \leq \varepsilon.$$

(iv) *([16], Theorem 6) Given a network architecture (L, \mathbf{p}) , there exists a positive constant $c(L)$ such that if $s \leq c(L)\varepsilon^{-1/(2L)}$, then*

$$\inf_{g \in \mathcal{F}(L, \mathbf{p}, s)} \|g - f\|_{\infty} \geq \varepsilon.$$

Part (iii) follows directly from Lemma 4.3. For (iv) one should notice that the number of hidden layers as defined in this work corresponds to $L-2$ in [16]. For each of the methods, Theorem 4.4 allows us to find a lower bound on the required number of parameters to achieve approximation error at least ε . For MARS and Faber-Schauder system, we need at least $O(\varepsilon^{-1/2})$ many parameters whereas there exist DNNs with $O(\log(1/\varepsilon))$ layers that require only $O(\log(1/\varepsilon))$ parameters.

Parts (i) and (ii) rely on the following classical result for the approximation by piecewise linear functions, which for sake of completeness is stated with a proof. Similar results have been used for DNNs by [16] and [9], Theorem 11.

Lemma 4.5. *Denote by $\mathcal{H}(K)$ the space of piecewise linear functions on $[0, 1]$ with at most K pieces and put $f(x) = x^2$. Then,*

$$\inf_{h \in \mathcal{H}(K)} \|h - f\|_{\infty} \geq \frac{1}{8K^2}.$$

Proof of Lemma 4.5. We prove this by contradiction assuming that there exists a function $h^* \in \mathcal{H}(K)$ with $\|h^* - f\|_\infty < 1/(8K^2)$. Because h^* consists of at most K pieces, there exist two values $0 \leq a < b \leq 1$ with $b - a \geq 1/K$ such that h^* is linear on the interval $[a, b]$. Using triangle inequality,

$$\begin{aligned} \left| h^*\left(\frac{a+b}{2}\right) - \left(\frac{a+b}{2}\right)^2 \right| &= \left| \frac{h^*(a) + h^*(b)}{2} - \left(\frac{a+b}{2}\right)^2 \right| \\ &\geq \left(\frac{a-b}{2}\right)^2 - \frac{1}{2}|h^*(a) - a^2| - \frac{1}{2}|h^*(b) - b^2| \\ &> \frac{1}{4K^2} - \frac{1}{8K^2} = \frac{1}{8K^2}. \end{aligned}$$

This is a contradiction and the assertion follows. \square

Proof of Theorem 4.4 (i) and (ii) : A univariate MARS function $f \in \mathcal{F}_{\text{MARS}}(M, C)$ is piecewise linear with at most $M + 1$ pieces. From Lemma 4.5 it follows that $\|f(x) - x^2\|_\infty \geq 1/(8(M + 1)^2) \geq 1/(36M^2)$. This yields (i). To prove (ii), observe that a univariate Faber-Schauder function $g \in \mathcal{F}_{\text{FS}}(M, C)$ is piecewise linear with at most 2^{M+2} pieces. (ii) thus follows again from Lemma 4.5.

The case $f(\mathbf{x}_1, \mathbf{x}_2) = (\mathbf{x}_1 + \mathbf{x}_2 - \mathbf{1})_+$: This function can be realized by a neural network with one layer and four parameters. Multivariate MARS functions and the Faber-Schauder system are, however, built by tensorization of the respective univariate basis functions. They are therefore not well-suited if the target function includes linear combinations over different inputs. Depending on the application this can indeed be a big disadvantage. To describe an instance where this happens consider a dataset with input being all pixels of an image. The machine learning perspective is that a canonical regression function depends on characteristic features of the underlying object such as edges in the image. Edge filters are discrete directional derivatives and therefore linear combinations of the input. This can easily be realized by a neural network but requires far more parameters if approximated by MARS or the Faber-Schauder system.

Lemma 4.6. For $f(x_1, x_2) = (x_1 + x_2 - 1)_+$ on $[0, 1]^2$,

$$\begin{aligned} (i) \quad & \inf_{h \in \mathcal{F}_{\text{MARS}}(M, \infty)} \|f - h\|_\infty \geq \frac{1}{8(M + 1)}; \\ (ii) \quad & \inf_{h \in \mathcal{F}_{\text{FS}}(M, \infty)} \|f - h\|_\infty \geq \frac{1}{8I}. \end{aligned}$$

Proof of Lemma 4.6. (i) Let $h \in \mathcal{F}_{\text{MARS}}(M, \infty)$. The univariate, piecewise linear function $h(\cdot, x_2) : [0, 1] \rightarrow \mathbb{R}$ has at most M breakpoints, where the locations of the breakpoints do not depend on x_2 (some breakpoints might, however, vanish for some x_2). Thus, there exist numbers $0 \leq a < b \leq 1$ with $b - a \geq 1/(M + 1)$, such that $h(\cdot, x_2)$ is linear in $[a, b]$ for all $x_2 \in [0, 1]$. Fix $x_2 = 1 - (a + b)/2$, such that

$$f(\cdot, x_2) = \sigma(\cdot - (a + b)/2).$$

In particular, $f(\cdot, x_2)$ is piecewise linear in $[a, b]$ with one breakpoint, and

$$f(a, x_2) = f((a+b)/2, x_2) = 0, \quad f(b, x_2) = (b-a)/2.$$

Therefore,

$$\sup_{x_1 \in [a, b]} |f(x_1, x_2) - h(x_1, x_2)| \geq \frac{b-a}{8} \geq \frac{1}{8(M+1)}.$$

(ii) Similar to (i) with $a = 0$ and $b = 2^{-M-1}$. \square

5 Risk comparison for nonparametric regression

In nonparametric regression with random design the aim is to estimate the dependence of a response variable $Y \in \mathbb{R}$ on a random vector $\mathbf{X} \in [0, 1]^d$ from i.i.d. noisy observations $(Y_i, \mathbf{X}_i)_{i=1, \dots, n}$ based on the model

$$Y_i = f_0(\mathbf{X}_i) + \varepsilon_i, \quad i = 1, \dots, n, \quad (6)$$

where $f_0 : [0, 1]^d \rightarrow [0, F]$ for some $F > 0$, and ε_i are assumed to be i.i.d. standard normal and independent of $(\mathbf{X}_i)_i$.

Consider optimization methods that converge to one of the local minima of the loss surface. [8] shows that if the activation function is linear, there are no poor local minima, that is, local minima with a larger loss than the global minimum. For non-linear activation function, there is a heuristic argument in [1] which states that the loss of all local minima lies in a band with size proportional to the geometric mean of the width vector. Moreover, the loss is obviously lower bounded by the loss of the global minimum. If this heuristic can be made rigorous, then any method that finds a local minimum over a class of neural networks \mathcal{F} will therefore return an estimator \hat{f} satisfying

$$\frac{1}{n} \sum_{i=1}^n (Y_i - \hat{f}(\mathbf{X}_i))^2 \leq \inf_{f \in \mathcal{F}} \frac{1}{n} \sum_{i=1}^n (Y_i - f(\mathbf{X}_i))^2 + \Delta_n, \quad (7)$$

where Δ_n is the width of the band. In particular, we recover the (global) empirical risk minimizer for $\Delta_n = 0$. Below, we study the estimator (7) over the DNN class $\mathcal{F}(L, \mathbf{p}, s)$. Notice that the least-squares loss is the intrinsic loss function induced by the log-likelihood of the nonparametric regression model. Therefore, it is the natural loss in this setting to fit a DNN (see also Section 6.2.1.1 in [6]). The performance is measured by the prediction risk

$$R(\hat{f}, f_0) := \mathbb{E}[(\hat{f}(\mathbf{X}) - f_0(\mathbf{X}))^2],$$

with \mathbf{X} having the same distribution as \mathbf{X}_1 but being independent of the sample $(Y_i, \mathbf{X}_i)_i$.

Theorem 5.1. Consider the d -variate nonparametric regression model (6) with bounded regression function f_0 . For any positive integer M , and any constant C , there exists a neural network class $\mathcal{F}(L, \mathbf{p}, s)$ with $L = O(\log Mn)$, $\max_\ell p_\ell = O(M)$ and $s = O(M \log Mn)$ such that the neural network estimator \hat{f} in (7) over the network class $\mathcal{F}(L, \mathbf{p}, s)$ satisfies

$$R(\hat{f}, f_0) \leq (1 + \gamma)^2 \left(\inf_{f \in \mathcal{F}_{\text{MARS}}(M, C)} \mathbb{E}[(f(\mathbf{X}) - f_0(\mathbf{X}))^2] + \Delta_n \right) + O\left(\frac{M \log^2(Mn) \log(M + 1)}{n\gamma}\right), \quad (8)$$

for all $\gamma \in (0, 1]$.

Theorem 5.1 gives an upper bound for the risk of the neural network estimator in terms of the best approximation over all MARS functions and a remainder. The remainder is roughly of order $\Delta_n + M/n$, where M is the maximal number of basis functions in $\mathcal{F}_{\text{MARS}}(M, C)$. If M is small the approximation term dominates. For large M , the remainder can be of larger order. This does, however, not imply that neural networks are outperformed by MARS. It is conceivable that the risk of the MARS estimator also include a variance term that scales with the number of parameters over the sample size and is therefore of order M/n . To determine an M that balances both terms is closely related to the classical bias-variance trade-off and depends on properties of the true regression function f . For a result of the same flavor, see Theorem 1 in [18]. A similar result also holds for the Faber-Schauder approximation.

Theorem 5.2. Consider the d -variate nonparametric regression model (6) with bounded regression function f_0 . For any positive integer M , and any constant C , there exists a neural network class $\mathcal{F}(L, \mathbf{p}, s)$ with $L = O(\log In)$, $\max_\ell p_\ell = O(I)$ and $s = O(I \log In)$ such that the neural network estimator \hat{f} in (7) over this network class satisfies

$$R(\hat{f}, f_0) \leq (1 + \gamma)^2 \left(\inf_{f \in \mathcal{F}_{\text{FS}}(M, C)} \mathbb{E}[(f(\mathbf{X}) - f_0(\mathbf{X}))^2] + \Delta_n \right) + O\left(\frac{I \log^2(In) \log(I + 1)}{n\gamma}\right),$$

for all $\gamma \in (0, 1]$.

6 Finite Sample Results

This section provides a simulation-based comparison of DNNs, MARS and expansion with respect to the Faber-Schauder system. The results complement the theoretical findings. We also consider higher-order MARS (HO-MARS) using the function system (2). In particular, we study frameworks in which the higher flexibility of networks yields much better reconstructions compared to the other approaches. For MARS we rely

on the py-earth package in Python, for DNNs we use the deep learning library Keras (Tensorflow backend) in Python.

The case $f_0(x) = x^2$: In the previous section, we have seen that MARS and Faber-Schauder system have worse approximation properties for the function $f_0(x) = x^2$ if compared with DNNs. It is therefore of interest to study this as a test case with simulated i.i.d. data from the model

$$Y_i = X_i^2 + \varepsilon_i, \quad X_i \sim \mathcal{U}[0, 1], \quad \varepsilon_i \sim \mathcal{N}(0, 0.2), \quad i = 1, \dots, 1000. \quad (9)$$

Since $f_0(x) = x^2$ is smooth, a good approximation should already be provided for a relatively small number of parameters in any of the considered function systems. Thus, we set $M = 10$ for MARS and $K = 3, M = 10$ for higher order MARS allowing for polynomials of degree up to three. For the Faber-Schauder class $\mathcal{F}_{FS}(M, C)$ we set $M = 3$ meaning that details up to size 2^{-3} can be resolved. For the neural network reconstruction, we consider dense networks with depth $L = 3$ and width $p_\ell = 3, \ell = 1, 2, 3$. The simulation results are summarized in Table 1, see also Figure 2. Concerning the prediction risk, all methods perform equally well, meaning that the effect of the additive noise in model (9) dominates the approximation properties of the function classes. In particular, we find that the smoothing steps of the backwards deletion procedure in the higher order MARS algorithm yield a piecewise linear approximation of the regression function and therefore, an incorrect classification of the polynomial degree of f_0 .

MARS	HO-MARS	FS	DNN
$4.01 \cdot 10^{-2}$ ($2 \cdot 10^{-3}$)	$4.00 \cdot 10^{-2}$ ($2 \cdot 10^{-3}$)	$3.99 \cdot 10^{-2}$ ($2 \cdot 10^{-3}$)	$4.03 \cdot 10^{-2}$ ($2 \cdot 10^{-3}$)
$2.89 \cdot 10^{-5}$ ($2 \cdot 10^{-6}$)	$< 10^{-26}$ ($< 10^{-25}$)	$1.34 \cdot 10^{-6}$ ($4 \cdot 10^{-8}$)	$1.54 \cdot 10^{-5}$ ($1 \cdot 10^{-5}$)

Table 1: Average prediction risks in models (9) (upper) and (10) (lower) based on 100 repetitions. Standard deviations in brackets.

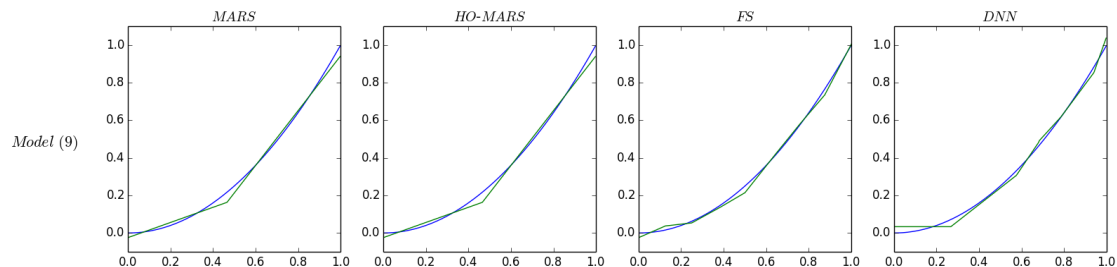


Figure 2: Reconstructions (green) in model (9). From left to right: MARS reconstruction with $M = 10$; higher order MARS reconstruction with $K = 3, M = 10$; Faber-Schauder reconstruction with $M = 3$; neural network reconstruction with architecture $L = 3, \mathbf{p} = (1, 3, 3, 3, 1)$. The regression function f_0 is depicted in blue.

It is natural to ask about the effect of the noise on the reconstruction in model (9). We therefore also study the same problem without noise, that is,

$$Y_i = X_i^2, \quad X_i \sim \mathcal{U}[0, 1], \quad i = 1, \dots, 1000. \quad (10)$$

The results are presented in Table 1, lower part. The higher order MARS reconstruction finds in this case the exact representation of the regression function. MARS, Faber-Schauder and neural networks result in a much smaller prediction risk if compared to the case with noise, and Faber-Schauder outperforms DNN estimation. This is in contrast to Theorem 4.4, which suggests that neural networks need much fewer parameters to approximate $f_0(x) = x^2$. Apparently, in this case the stochastic gradient descent finds a reconstruction that has much fewer linear pieces than the optimal approximation with a neural network of this architecture. We find that the reconstruction strongly depends on the initialization of the network and investigate this effect in Table 2. For every dataset, $k \in \{1, 5, 10, 25\}$ networks with different random initializations are trained, and the prediction risk is reported for the network which minimizes the loss function. The prediction risk decreases as k increases. The higher standard deviation in the case $k = 25$ compared to, e.g., the MARS representation in Table 1 suggests that increasing k even more might be beneficial. This is, however, computationally costly.

$k = 1$	$k = 5$	$k = 10$	$k = 25$
$4.68 \cdot 10^{-2}$	$1.97 \cdot 10^{-3}$	$5.84 \cdot 10^{-5}$	$1.54 \cdot 10^{-5}$
$(4 \cdot 10^{-2})$	$(1 \cdot 10^{-2})$	$(1 \cdot 10^{-4})$	$(1 \cdot 10^{-5})$

Table 2: Average prediction risks in model (10) based on 100 repetitions. Standard deviations in brackets. Reported risks are for networks which minimize the loss over k random initializations for the same dataset.

The case $f_0(\mathbf{x}) = \sin(5 \cdot 2\pi\mathbf{x})$: To compare the different methods for rough functions, we simulate i.i.d. data from

$$Y_i = \sin(5 \cdot 2\pi X_i), \quad X_i \sim \mathcal{U}[0, 1], \quad i = 1, \dots, 1000. \quad (11)$$

For such highly oscillating functions, all methods require many parameters. Therefore we study MARS with $M = 50$, higher order MARS with $K = 5$ and $M = 50$, the Faber-Schauder system with $M = 6$ and fully-connected networks with number of hidden layers $L = 15$ and network width vector $\mathbf{p} = (1, 10, \dots, 10, 1)$. Results are displayed in Table 3 and Figure 3. In this case the Faber-Schauder expansion performs best.

MARS	HO-MARS	FS	DNN
$2.25 \cdot 10^{-3}$ ($4 \cdot 10^{-4}$)	$9.70 \cdot 10^{-4}$ ($4 \cdot 10^{-4}$)	$3.94 \cdot 10^{-5}$ ($2 \cdot 10^{-6}$)	$1.91 \cdot 10^{-3}$ ($2 \cdot 10^{-3}$)
$6.06 \cdot 10^{-4}$ ($4 \cdot 10^{-4}$)	$2.64 \cdot 10^{-4}$ ($2 \cdot 10^{-4}$)	$2.08 \cdot 10^{-3}$ ($5 \cdot 10^{-4}$)	$2.14 \cdot 10^{-3}$ ($1 \cdot 10^{-3}$)

Table 3: Average prediction risks in models (11) (upper) and (12) (lower) based on 100 repetitions. Standard deviations in brackets.

The case $f_0(\mathbf{x}) = -1/2 + \mathbb{1}(\mathbf{x} \geq 1/2)$: As another toy example we consider regression with a jump function to investigate the approximation performance in a setup in which standard smoothness assumptions are violated. For this we generate i.i.d. data from

$$Y_i = \begin{cases} -\frac{1}{2}, & \text{if } X_i < \frac{1}{2}, \\ \frac{1}{2}, & \text{if } X_i \geq \frac{1}{2}, \end{cases} \quad X_i \sim \mathcal{U}[0, 1], \quad i = 1, \dots, 1000. \quad (12)$$

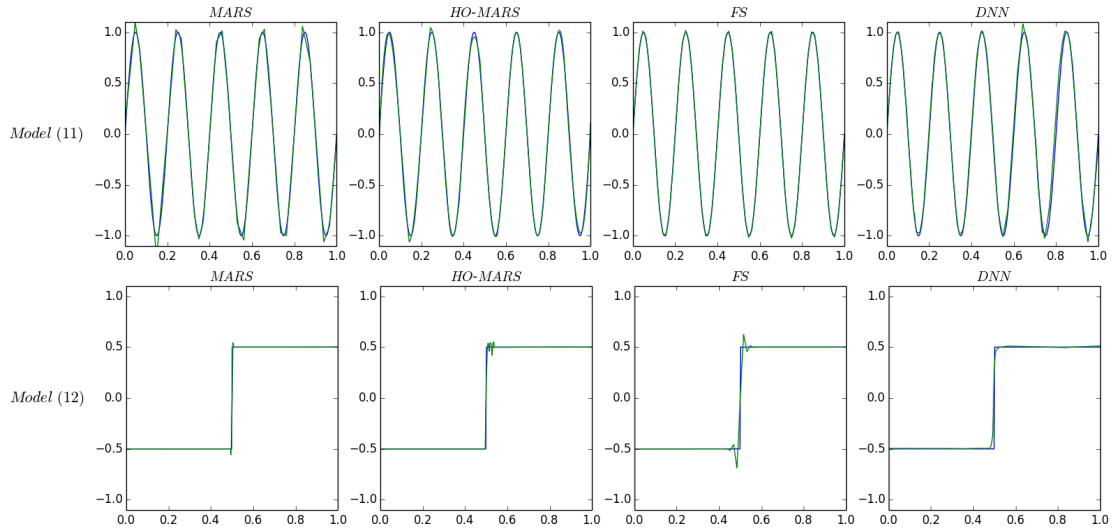


Figure 3: Reconstructions (green) in model (11) (upper) and model (12) (lower). From left to right: MARS reconstruction with $M = 50$; higher order MARS reconstruction with $K = 5, M = 50$; Faber-Schauder reconstruction with $M = 6$; neural network reconstruction with architecture $L = 15, \mathbf{p} = (1, 10, \dots, 10, 1)$. f_0 is depicted in blue.

We use the same choices of parameters as in the simulation before. Results are shown in Table 3 and Figure 3, lower parts. Compared with the other methods, the neural network reconstruction does not add spurious artifacts around the jump location.

The case $f_0(\mathbf{x}_1, \mathbf{x}_2) = (\mathbf{x}_1 + \mathbf{x}_2 - 1)_+$: By Lemma 4.6, this function is an example of a function for which DNNs need much fewer parameters than MARS or the Faber-Schauder system. We generate i.i.d. data from

$$Y_i = (X_{i,1} + X_{i,2} - 1)_+, \quad \mathbf{X}_i = (X_{i,1}, X_{i,2})^\top \sim \mathcal{U}[0, 1]^2, \quad i = 1, \dots, 1000. \quad (13)$$

Notice that the regression function f_0 is piecewise linear with change of slope along the line $x_1 + x_2 = 1$, $\mathbf{x} = (x_1, x_2)^\top \in [0, 1]^2$. For convenience we only consider the more flexible higher order MARS. The prediction risks reported in Table 4 and the reconstructions displayed in Figure 4 show that in this problem shallow neural networks outperform higher order MARS and reconstruction with respect to the Faber-Schauder system even if we allow for more parameters.

HO-MARS	FS	DNN
$2.20 \cdot 10^{-4}$ ($7 \cdot 10^{-5}$)	$9.86 \cdot 10^{-5}$ ($9 \cdot 10^{-6}$)	$7.13 \cdot 10^{-7}$ ($1 \cdot 10^{-6}$)

Table 4: Average prediction risks in model (13) based on 100 repetitions. Standard deviations in brackets.

Dependence on input dimension: In this simulation the risk dependence on the

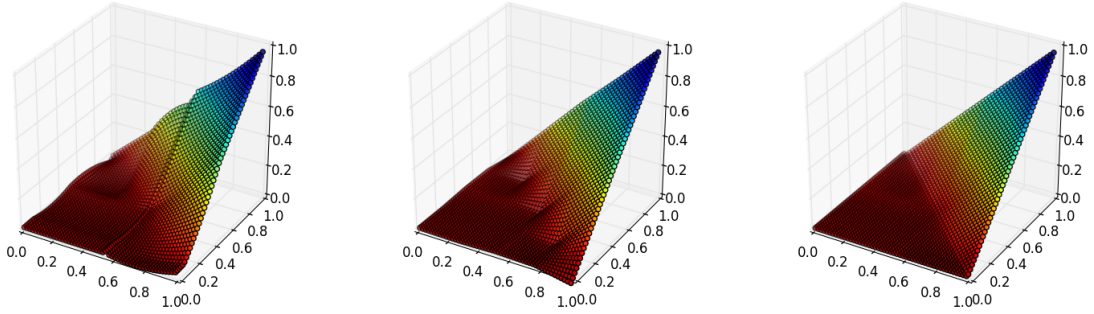


Figure 4: *Reconstructions in model (13). From left to right: Higher order MARS with $K = 10$, $M = 20$; Faber-Schauder reconstruction for $M = 2$; neural network reconstruction for $L = 1$, $\mathbf{p} = (2, 1, 1)$.*

dimension is investigated. We generate i.i.d. data from

$$\mathbf{Y}_i = \left(\sum_{j=1}^d X_{i,j}^2 - \frac{d}{3} \right)_+, \quad \mathbf{X}_i = (X_{i,1}, \dots, X_{i,d})^\top \sim \mathcal{U}[0, 1]^d, \quad i = 1, \dots, 1000. \quad (14)$$

This function is constructed in such a way that it can be well-approximated by both higher order MARS and neural networks. Independently of the dimension d the setup for higher order MARS is $K = 10$ and $M = 30$. We choose a densely connected neural network with architecture $L = 15$, $\mathbf{p} = (d, 10, \dots, 10, 1)$. The risks for $d = 1, 2, 5, 10$ are summarized in Table 5. The result shows that both methods suffer from the curse of dimensionality. Neural networks achieve a consistently smaller risk for all dimensions.

	HO-MARS		DNN	
$d = 1$	$1.47 \cdot 10^{-5}$	$(3 \cdot 10^{-6})$	$1.33 \cdot 10^{-6}$	$(4 \cdot 10^{-6})$
$d = 2$	$1.87 \cdot 10^{-4}$	$(4 \cdot 10^{-5})$	$3.21 \cdot 10^{-5}$	$(3 \cdot 10^{-5})$
$d = 5$	$8.40 \cdot 10^{-3}$	$(9 \cdot 10^{-4})$	$1.89 \cdot 10^{-3}$	$(9 \cdot 10^{-4})$
$d = 10$	$5.83 \cdot 10^{-2}$	$(3 \cdot 10^{-3})$	$1.52 \cdot 10^{-2}$	$(2 \cdot 10^{-3})$

Table 5: *Average prediction risks in model (14) based on 100 repetitions. Standard deviations in brackets.*

To study the approximation performance for large input dimensions we consider i.i.d. data from the model

$$\mathbf{Y}_i = \left(\sum_{j=1}^{10} X_{i,j}^2 - \frac{10}{3} \right)_+, \quad \mathbf{X}_i = (X_{i,1}, \dots, X_{i,d})^\top \sim \mathcal{U}[0, 1]^d, \quad i = 1, \dots, 1000. \quad (15)$$

Here, the number of active parameters 10 is fixed and small in comparison to the input dimension. For $d = 1000$ the input dimension is the same as the sample size. We consider higher order MARS and neural networks with the same parameters as before. The risks are summarized in Table 6. They are comparable with the results in the last row of Table 5 showing that both neural network and higher order MARS estimates are adaptive with respect to the active parameters of the model.

	HO-MARS		DNN	
$d = 100$	$5.81 \cdot 10^{-2}$	$(3 \cdot 10^{-3})$	$1.32 \cdot 10^{-2}$	$(3 \cdot 10^{-3})$
$d = 1000$	$5.68 \cdot 10^{-2}$	$(4 \cdot 10^{-3})$	$3.73 \cdot 10^{-3}$	$(2 \cdot 10^{-3})$

Table 6: Average prediction risks in model (15) based on 100 repetitions. Standard deviations in brackets.

7 Proofs

Proof of Lemma 4.1: We first consider the approximation of one basis function h_m for fixed $m \in \{1, \dots, M\}$ by a network. By (1), each function h_m has the representation

$$h_m(\mathbf{x}) = \prod_{j \in I} (s_j(x_j - t_j))_+$$

for some index set $I \subseteq \{1, \dots, d\}$, sign vectors $s_j \in \{-1, 1\}$ and shifts $\mathbf{t} = (t_j)_{j \in I} \in [0, 1]^{|I|}$.

Now we use Lemma 4.3 to construct a network

$$H_{m,N} \in \mathcal{F}((N+5)\lceil \log_2 d \rceil + 1, (d, d, 6d, 6d, \dots, 6d, 1), s)$$

such that $\|H_{m,N} - h_m\|_\infty \leq 3^d 2^{-N}$. The first hidden layer of the network $H_{m,N}$ builds the factors $(s_j(x_j - t_j))_+$ for the input $\mathbf{x} \in \mathbb{R}^d$. The remaining $d - |I|$ terms of the first layer are set to one. This can be achieved by choosing the first weight matrix to be $W_1 = (s_j \mathbb{1}(i = j, i \in I))_{i,j \in \{1, \dots, d\}}$ and the corresponding shift vector as $\mathbf{v}_1 = (s_j t_j \mathbb{1}(j \in I) - \mathbb{1}(j \notin I))_j$, where $\mathbb{1}(\cdot)$ denotes the indicator function.

Because of $(s_j(x_j - t_j))_+ \in [0, 1]$ for $\mathbf{x} \in [0, 1]^d$, the multiplication network Mult_N^d introduced in Lemma 4.3 can be applied to the first layer of the network. The resulting network $H_{m,N}$ is then in the class

$$\mathcal{F}((N+5)\lceil \log_2 d \rceil + 1, (d, d, 6d, \dots, 6d, 1), s)$$

and satisfies $\|H_{m,N} - h_m\|_\infty \leq 3^d 2^{-N}$. The number of active parameters of the network $H_{m,N}$ is $s \leq 42d^2((N+5)\lceil \log_2 d \rceil + 2)$.

We can simultaneously generate the networks $H_{m,N}$, $m = 1, \dots, M$, in the network space $\mathcal{F}((N+5)\lceil \log_2 d \rceil + 1, (d, Md, 6Md, \dots, 6Md, M), Ms)$. Finally, we describe the construction of a network h that approximates the function $f = \beta_0 + \sum_{m=1}^M \beta_m h_m$ with all coefficients bounded in absolute value by C . For that we first include a layer that maps $(h_1, \dots, h_M)^\top$ to $(1, h_1, \dots, h_M)^\top$ using $M+1$ active parameters. Every component is then multiplied with C by parallelized sub-networks with width 2, $2\lceil \log_2 C \rceil - 1$ hidden layers and $4\lceil \log_2 C \rceil$ parameters each. It is straightforward to construct such a sub-network.

For the last layer we set $W_{L+1} = C^{-1}(\beta_m)_m$. Setting $N \geq \log_2(C(M+1)3^d/\varepsilon)$ the approximation error is

$$\|h - f\|_\infty \leq C(M+1)3^d 2^{-N} \leq \varepsilon.$$

The number of active parameters of h is

$$M42d^2((N+5)\lceil\log_2 d\rceil + 2) + 2 + M(4\lceil\log_2 C\rceil + 2).$$

Moreover, $L = (N+5)\lceil\log_2 d\rceil + 2\lceil\log_2 C\rceil + 3$ and $\max_{\ell=0,\dots,L+1} p_\ell \leq 6Md$. \square

Proofs of Theorem 5.1 and Theorem 5.2: We derive an upper bound for the risk of the empirical risk minimizer using the following oracle inequality, which was proven in [13]. Let $\mathcal{N}(\delta, \mathcal{F}, \|\cdot\|_\infty)$ be the covering number, that is, the minimal number of $\|\cdot\|_\infty$ -balls with radius δ that covers \mathcal{F} (the centers do not need to be in \mathcal{F}).

Lemma 7.1 (Lemma 8 in [13]). *Consider the d -variate nonparametric regression model (6) with unknown regression function f_0 . Let \hat{f} be any estimator satisfying (7) for some Δ_n and $\{f_0\} \cup \mathcal{F} \subset \{f : [0, 1]^d \rightarrow [0, F]\}$ for some $F \geq 1$. If $\mathcal{N}_n := \mathcal{N}(\delta, \mathcal{F}, \|\cdot\|_\infty) \geq 3$, then,*

$$R(\hat{f}, f) \leq (1 + \gamma)^2 \left[\inf_{f \in \mathcal{F}} \mathbb{E}[(f(\mathbf{X}) - f_0(\mathbf{X}))^2] + \Delta_n + F^2 \frac{14 \log \mathcal{N}_n + 20}{n\gamma} + 26\delta F \right],$$

for all $\delta, \gamma \in (0, 1]$.

Using the Lipschitz-continuity of the ReLU function, the covering number of a network class can be bounded as follows.

Lemma 7.2 (Lemma 10 in [13]). *If $V := \prod_{\ell=0}^{L+1} (p_\ell + 1)$, then, for any $\delta > 0$,*

$$\log \mathcal{N}(\delta, \mathcal{F}(L, \mathbf{p}, s), \|\cdot\|_\infty) \leq (s+1) \log \left(2\delta^{-1}(L+1)V^2 \right).$$

Proof of Theorem 5.1. Given (M, C) with C fixed, there exists by Lemma 4.1 a network class $\mathcal{F}(L, \mathbf{p}, s)$ such that $L = O(\log Mn)$, $\max_\ell p_\ell = O(M)$, $s = O(M \log Mn)$ and such that $\inf_{h \in \mathcal{F}(L, \mathbf{p}, s)} \|h - f\|_\infty \leq 1/n$. We will show that for this class, (8) holds.

We bound the metric entropy using Lemma 7.2. For two positive sequences \lesssim means that the right hand side is bounded by the left hand side up to a multiplicative constant. Observe that

$$\log V = \log \left(\prod_{\ell=0}^{L+1} (p_\ell + 1) \right) \lesssim L \log \left(\max_{\ell=0,\dots,L+1} p_\ell \right) \lesssim L \log(M+1)$$

yields the upper bound

$$\begin{aligned} \log \mathcal{N} \left(\frac{1}{n}, \mathcal{F}(L, \mathbf{p}, s), \|\cdot\|_\infty \right) &\lesssim M \log(Mn) \left(\log(4nL) + L \log(M+1) \right) \\ &\lesssim M \log^2(Mn) \log(M+1). \end{aligned}$$

Lemma 7.1 and an application of Lemma 4.1 finally yield the assertion

$$\begin{aligned}
& R(\hat{f}, f_0) \\
& \leq (1 + \gamma)^2 \left(\inf_{f \in \mathcal{F}(L, \mathbf{p}, s)} \mathbb{E}[(f(\mathbf{X}) - f_0(\mathbf{X}))^2] + \Delta_n \right) + O\left(\frac{M \log^2(Mn) \log(M + 1)}{n\gamma}\right) \\
& \leq (1 + \gamma)^2 \left(\inf_{f \in \mathcal{F}_{\text{MARS}}(M, C)} \mathbb{E}[(f(\mathbf{X}) - f_0(\mathbf{X}))^2] + \Delta_n \right) + O\left(\frac{M \log^2(Mn) \log(M + 1)}{n\gamma}\right).
\end{aligned}$$

□

Proof of Theorem 5.2. By replacing M and I in the bounds, the proof can be derived in the same way as the proof of Theorem 5.1. □

References

- [1] CHOROMANSKA, A., HENAFF, M., MATHIEU, M., AROUS, G. B., AND LECUN, Y. The loss surface of multilayer networks. *Aistats* (2015), 192–204.
- [2] ELKAN, R., AND SHAMIR, O. The power of depth for feedforward neural networks. *ArXiv Preprint* (2017).
- [3] FABER, G. Über die Orthogonalfunktionen des Herrn Haar. *Jahresbericht der Deutschen Mathematiker-Vereinigung 19* (1910), 104–112.
- [4] FRIEDMAN, J. H. Multivariate adaptive regression splines. *Ann. Statist.* 19, 1 (1991), 1–141.
- [5] FRIEDMAN, J. H. Fast mars. Tech. rep., Stanford University Department of Statistics, Technical Report 110, 1993.
- [6] GOODFELLOW, I., BENGIO, Y., AND COURVILLE, A. *Deep Learning*. MIT Press, 2016.
- [7] HASTIE, T., TIBSHIRANI, R., AND FRIEDMAN, J. *The Elements of Statistical Learning*, second ed. Springer, New York, 2009.
- [8] KAWAGUCHI, K. Deep learning without poor local minima. In *Advances in Neural Information Processing Systems 29*. Curran Associates, 2016, pp. 586–594.
- [9] LIANG, S., AND SRIKANT, R. Why Deep Neural Networks for Function Approximation? *ArXiv e-prints* (2016).
- [10] MHASKAR, H. N. Approximation properties of a multilayered feedforward artificial neural network. *Advances in Computational Mathematics 1*, 1 (1993), 61–80.

- [11] NEEDELL, D., WARD, R., AND SREBRO, N. Stochastic gradient descent, weighted sampling, and the randomized Kaczmarz algorithm. In *Advances in Neural Information Processing Systems 27*. Curran Associates, 2014, pp. 1017–1025.
- [12] POGGIO, T., MHASKAR, H., ROSASCO, L., MIRANDA, B., AND LIAO, Q. Why and when can deep-but not shallow-networks avoid the curse of dimensionality: A review. *International Journal of Automation and Computing* 14, 5 (2017), 503–519.
- [13] SCHMIDT-HIEBER, J. Nonparametric regression using deep neural networks with ReLU activation function. *ArXiv e-prints* (2017).
- [14] TELGARSKY, M. Benefits of depth in neural networks. *ArXiv Preprint* (2016).
- [15] VAN DER MEULEN, F., SCHAUER, M., AND VAN WAAIJ, J. Adaptive nonparametric drift estimation for diffusion processes using Faber–Schauder expansions. *Statistical Inference for Stochastic Processes* (2017).
- [16] YAROTSKY, D. Error bounds for approximations with deep ReLU networks. *Neural Networks* 94 (2017), 103 – 114.
- [17] ZHANG, Y., LEE, J. D., AND JORDAN, M. I. L1-regularized neural networks are improperly learnable in polynomial time. In *ICML'16* (2016), pp. 993–1001.
- [18] ZHANG, Y., LIANG, P., AND WAINWRIGHT, M. J. Convexified convolutional neural networks. In *PMLR* (2017), vol. 70, pp. 4044–4053.